RSC Advances

ROYAL SOCIETY OF CHEMISTRY

www.rsc.org/advances

ToC graphic and synopsis

Tetraphenylethylenes in which one or two of the core phenyl rings have been replaced with pyridine or pyridinium groups have been prepared and evaluated as aggregation-induced emission fluorophores

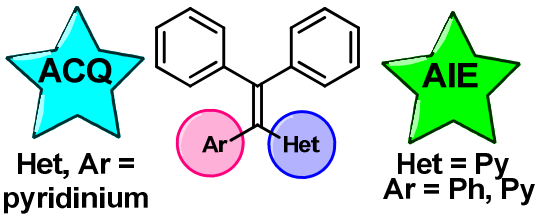

Journal Name

ARTICLE

Synthesis and aggregation-induced emission properties of pyridine and pyridinium analogues of tetraphenylethylene

Received 00th January 20xx,
Accepted 00th January 20xx

DOI: 10.1039/x0xx00000x

www.rsc.org/

Moustafa T. Gabr and F. Christopher Pigge*

Aggregation-induced emission (AIE) is emerging as an important design element in a variety of new fluorescent-based chemical sensors and bio-imaging agents. In particular, derivatives of tetraphenylethylene (TPE) have been widely utilized in this regard as the TPE framework is a reliable AIE-luminogen. To expand the library of AIE active tetraarylethylenes, we have explored the effects of replacing one or two of the phenyl rings in TPE with pyridine. Efficient synthetic routes that deliver mono- and bis-pyridyl tetraarylethylenes have been developed and the luminescent properties of these heterocyclic TPE analogues, along with their corresponding N-methylated pyridinium salts, have been examined.

Introduction

Organic fluorophores play important roles in chemical biology and materials science. Conjugation of organic dyes to various biomolecules and ligands provides a means to probe enzymatic and cellular processes using fluorescence spectroscopy.[1] Likewise, organic fluorophores are fundamental components in several types of functional materials, such as organic light-emitting diodes (OLED) and fluorescent sensors.[2]

Conventional organic fluorophores typically operate most efficiently under high-dilution conditions, and fluorescence quenching is observed in concentrated solution and the solid state. This feature limits the conditions under which most fluorescent organic compounds can be effectively utilized. Certain classes of organic molecules, however, display the opposite behavior. These compounds exhibit little to no fluorescence in dilute solution, but become markedly more fluorescent when aggregated or in the solid state. The term "aggregation induced emission" (AIE) has been introduced by Tang to describe this behavior, and compounds exhibiting this property are said to be AIE-active fluorophores.[3]

Although several different types of compounds have been identified as AIE active, the most widely used AIE luminogens in bio- and materials science are derivatives of tetraphenylethylene (TPE, **1**, Figure 1).[4] Functionalized TPEs are often non-emissive when dissolved in good solvents, but display a fluorescent signal when combined with poor solvents or upon precipitation/crystallization. The basis for this fluorescence response is believed to reside in restriction of intramolecular motion (e.g., rotations about the phenyl – ethylene bonds) that occurs upon aggregation.[3b,5] This property of TPEs has been harnessed as the operative design element in a number of chemical and biochemical fluorescent sensors and detectors.[3,4] In particular, incorporation of one or more pyridine rings into the periphery of the TPE core has produced several intriguing AIE-active materials. For example, an N-benzylated derivative of (4-pyridyl)TPE **2** possessing a reactive boronic ester exhibits fluorescence turn-on detection of H_2O_2 and glucose in aqueous solution.[6] Additionally, N-methylpyridinium salts of **2** have been shown to display tunable emission in the solid state as a function of counteranion.[7] The 4-vinylpyridyl-functionalized TPE **3** has shown efficacy as a sensing agent for trivalent cations (e.g., Fe^{3+}),[8] while simple alkylpyridinium salts prepared from **3** show selective fluorescence response in the presence of pyrophosphate anion.[9] Other derivatives of **3** have been used for fluorescence bioimaging (e.g., monitoring of targeted drug delivery and cell apoptosis)[10] as well as mitochondrial staining.[11] Bis(4-vinylpyridyl)TPE **4** has been used as monomer in construction of polycationic polymers for detection of heparin,[12] while the dimethylpyridinium salt displays interesting mechanochromic properties.[13] Finally, the tetra(4-pyridyl)TPE **5** has been employed in a number of AIE active constructs, including pH sensitive fluorescence indicators[14] and supramolecular polymers.[15] TPE **5** also exhibits selective detection of $Hg(HSO_4)_2$,[16] and has been demonstrated to be an excellent halogen bond acceptor in mediating assembly of crystalline fluorescent halogen bonded networks with iodoarenes.[17] The tetratopic array of pyridine groups in **5** has also been harnessed in construction of metal-organic as well as main group-organic coordination polymers,[18] and in assembly of dynamic supramolecular coordination complexes.[19]

A common feature shared by TPE derivatives **2**-**5** is the attachment of one or more pyridine rings to the periphery of the TPE core. In part, this reflects the accessibility of functionalized TPEs to which heterocyclic arenes (such as pyridine or vinylpyridine) can be readily attached. Only a handful of tetraarylethylene (TAE) analogues of TPE in which one of the core phenyl rings has been replaced with pyridine (e.g., **6**) have been reported, and the photophysical properties of these compounds have not been examined.[20] Indeed, examples of tetraarylethylenes with other heterocyclic arenes (such as furan, thiophene, and pyrrole) are also rare.[21] Given

Department of Chemistry, University of Iowa, Iowa City, Iowa, 52242, USA

Electronic Supplementary Information (ESI) available: absorption and fluorescence spectra, NMR spectra, crystallographic data, cif files. See DOI: 10.1039/x0xx00000x

the broad utility of pyridyl-functionalized TPEs **2**-**5** in diverse areas of supramolecular chemistry, it is anticipated that compounds such as **6** and closely related congeners also should exhibit desirable fluorescent properties while retaining considerable synthetic flexibility for additional elaboration. Moreover, direct replacement of phenyl with pyridine results in TAE derivatives with smaller molecular footprints relative to **2**-**5** and potentially greater hydrophilicities, issues that are important in biological applications. Thus, we report here a new synthesis of **6** along with several other mono- and bis(pyridyl) tetraarylethylenes. Since much of the utility of **2**-**5** derives from N-alkylated derivatives, pyridyl tetraarylethylenes prepared in this study were also converted to their associated N-methylpyridinium tetrafluoroborate salts. These novel heterocyclic TPE-inspired materials have been further characterized by fluorescence spectroscopy.

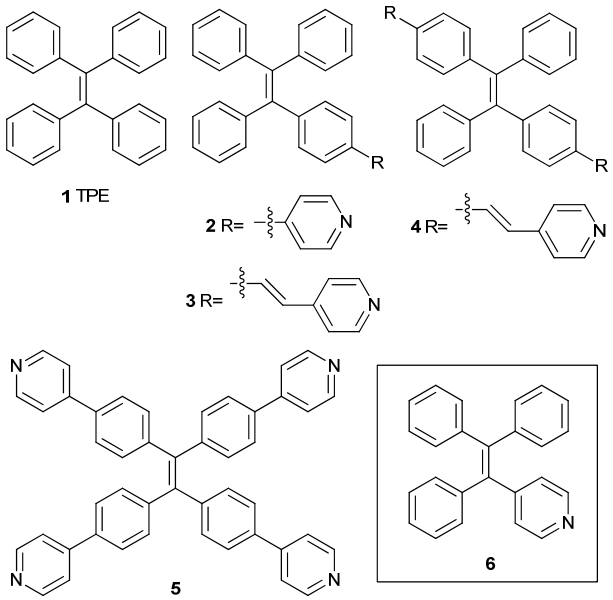

Fig. 1. Examples of pyridine-functionalized TPEs (**2**-**5**).

Results and Discussion

To access the initial targets of this investigation (triphenyl vinylpyridines **6**-**8** or TPVPs) we adopted an approach that has proven successful in construction of conventional tetraphenylethylenes. As illustrated in Scheme 1, the lithium anion derived from trimethylsilyl-substiuted diphenylmethane was condensed with a series of isomeric phenyl pyridyl ketones (pyridyl = 4-pyridyl, 3-pyridyl, or 2-pyridyl) to effect Peterson olefination.[22] The TPVP derivatives **6**-**8** were obtained in comparable yields. Notably, condensation of diphenylmethane with the same phenyl pyridyl ketones followed by acid-catalyzed (p-TSA) dehydration of the putative carbinol products delivered **6**-**8** in significantly lower yields.[23] The presence of the desired pyridine-containing TAE products was qualitatively indicated by the appearance of long wavelength fluorescent material in TLC analysis of crude reaction mixtures. Each TPVP derivative was then converted to the corresponding N-methylpyridinium salt in good yield.

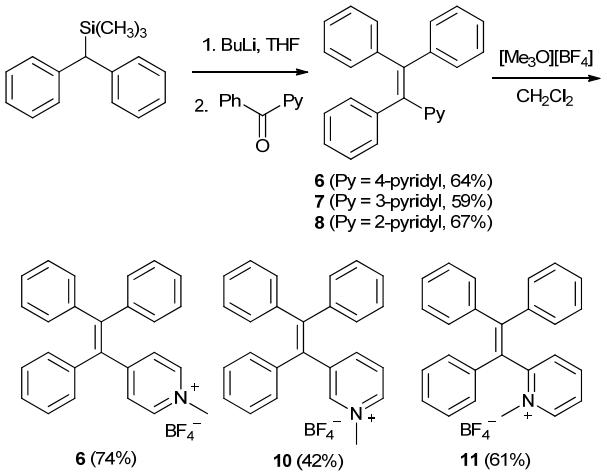

Scheme 1. Synthesis of TPVPs **6**-**8** and their corresponding N-methylpyridinium salts.

The preparative route shown in Scheme 1 works well for construction of unsubstituted TPVPs, however, we found an alternate route involving Suzuki coupling to be more effective for preparation of substituted TPVPs bearing electron donating groups (e.g., OMe) as illustrated in Scheme 2. 4-Pyridyl phenyl ketone **12** was converted to the geminal dibromoalkene **13** by treatment with CBr_4 and PPh_3. Double Suzuki coupling was then used to install methoxyphenyl groups in the tetraarylethylene framework, affording **14** in good overall yield. Although not typically used to construct tetraarylethylenes, the advantages of similar Suzuki coupling strategies in accessing unsymmetrical tetraphenylethylenes that would be difficult to prepare by other methods has been noted.[24] The pyridyl group in **14** was also easily methylated to give **15**.

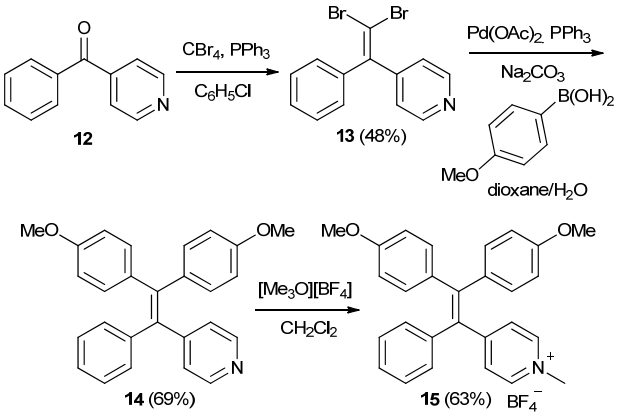

Scheme 2. Double Suzuki coupling for synthesis of substituted TPVP derivatives.

Double Suzuki coupling was also employed to construct two representative examples of 1,1-diphenyl-2,2-dipyridylethylenes (DPDPyEs). In these examples the known dibromoalkene[25] **16** was coupled with either 3- or 4-pyridyl boronic acid (Scheme 3). Coupling proceeded smoothly in each case, and the DPDPyE derivatives **18** and **19** were isolated in serviceable yields. Treatment of each dipyridylethylene with an excess of

$[Me_3O][BF_4]$ in methanol afforded the bis(pyridinium) salts **20** and **21**.

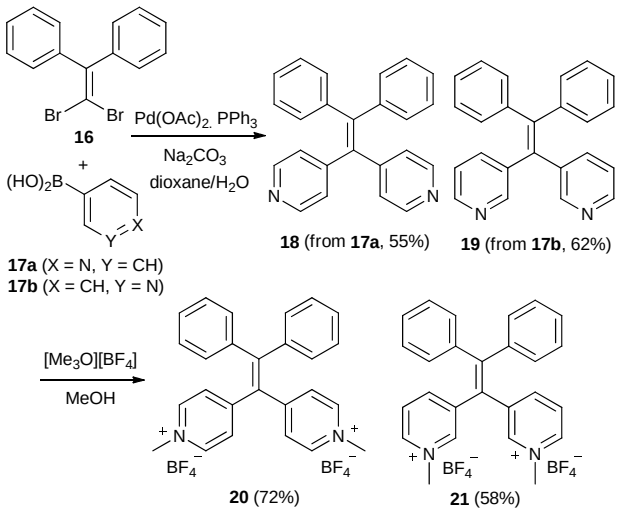

Scheme 3. Synthesis of diphenyl dipyridyl ethylenes (DPDPyEs).

X-Ray quality single crystals of two compounds described above (**14** and **18**) were obtained from slow evaporation of EtOAc/MeOH solutions.[26] Their respective molecular structures are shown in Figs. 2-3. In each case the four aryl rings are arrayed in propeller-like fashion around the central ethylene linkage. The torsion angles of the four arenes with respect to the ethylene bond in **14** range from ~44° to ~62°, while the range of torsion angles in **18** is somewhat narrower (51-61°). In **14**, individual molecules are part of extended helical assemblies, facilitated in part by solid state C–H···N hydrogen bonding between the pyridine nitrogen and a C–H group from a methoxy substituent (see ESI). The extended packing in **18** features an ABAB-type layer structure down *c* with adjacent interlayer DPDPyE molecules rotated ~180° (ESI).

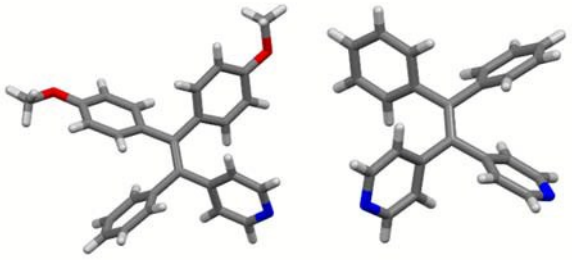

Fig. 2. Molecular structure of TPVP **14** (left) and DPDPyE **18** (right).

The TPVPs **6**-**8** exhibited similar UV-visible absorption spectra in CH_3CN solution. Each compound displayed a relatively featureless absorption spectrum with longest wavelength absorption at ~ 340 nm (see ESI). In contrast, **6**-**8** did display significant differences in their fluorescence spectra under conditions leading to aggregation induced emission. For example, the fluorescence spectrum of **6** in 100% CH_3CN (a medium in which **6** is readily soluble) revealed only minimal emission. However, incremental addition of H_2O (a poor solvent for **6**) induced a markedly red-shifted fluorescence response with λ_{em} ~ 455 nm (Figure 3a). Aggregation induced emission effects observed in isomeric TPVPs **7** and **8** under similar conditions (CH_3CN/H_2O) were much less pronounced (Figures 3b,c), and the $\lambda_{max,em}$ of 3-pyridyl isomer **7** appears blue-shifted compared to the 4- and 2-pyridyl analogues **6** and **8**. This presumably reflects the more pronounced electron-withdrawing abilities of the substituted pyridines in these latter two TPVPs. The differences in AIE effect among TPVP isomers is further illustrated by comparing plots of relative fluorescence enhancement (I/I_o) as a function of water fraction (f_{H2O}) in CH_3CN solvent. As illustrated in Fig. 3d, 4-pyridyl-TPVP **6** displays the greatest aggregation-induced fluorescence enhancement, while the 2-pyridyl derivative **8** exhibits only minimal changes in fluorescence intensity. Clearly, the position of the nitrogen atom within the TPVP framework influences the luminescent properties of these materials. The most noticeable departure from typical AIE behavior is exhibited by 2-pyridyl isomer **8**, as this material displays essentially constant fluorescence irrespective of aggregation state. We speculate that replacement of a C-H group with the pyridine nitrogen atom may result in reduced steric interactions between the 2-pyridyl ring and adjacent phenyl rings, in turn leading to greater pyridine-ethylene π-orbital overlap and fluorescence emission from both monomers and aggregated oligomers.

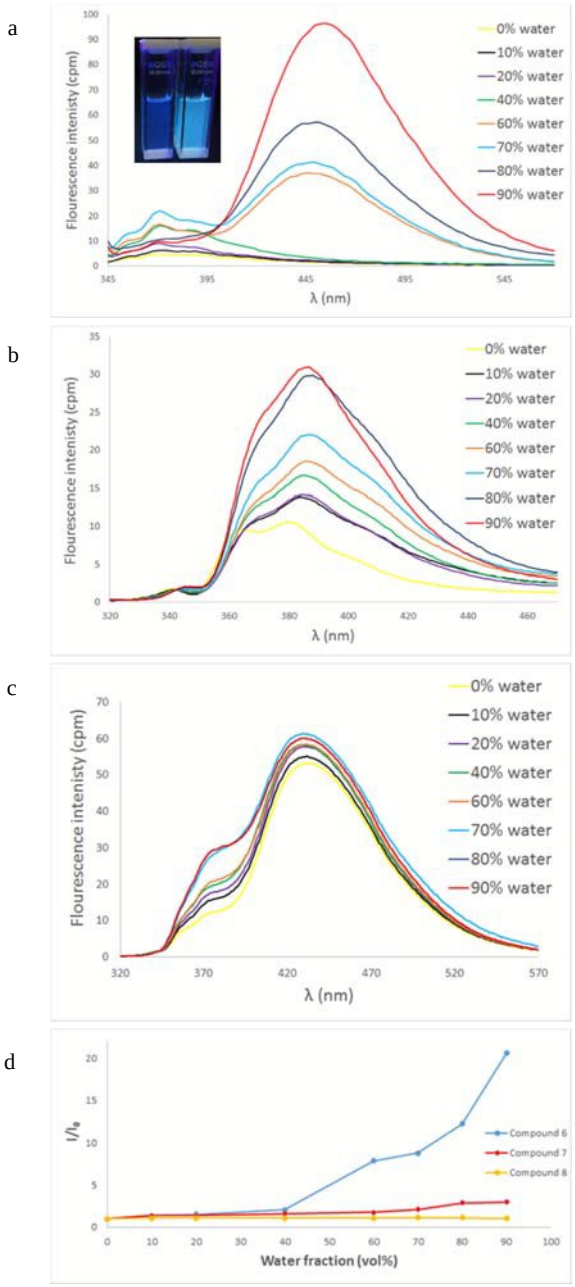

Fig. 3. (a) Fluorescence spectra of **6** in CH_3CN/H_2O mixture. Inset: Picture taken under UV light of **6** in 100% CH_3CN (left) and 90:10 H_2O:CH_3CN (right). (b) Fluorescence spectra of **7** in CH_3CN/H_2O mixture. (c) Fluorescence spectra of **8** in CH_3CN/H_2O mixture. (d) Plot of relative emission intensity (I/I_o) vs. H_2O fraction (vol%) for **6**-**8**. I_o = emission intensity in 100% CH_3CN. Sample concentration 10 μM and λex = 305 nm in each case.

Several pyridinium-substituted TPE's derived from neutral precursors **2**-**5** (Fig. 1) have been found to possess interesting photoluminescent properties,[7,9,11,13] thus, TPVPs **6**-**8** were each converted to pyridinium salts to probe the effects of pyridinium ion formation on absorbance and emission in this system. Conversion of the neutral TPVP isomers **6**-**8** to the corresponding N-methyl pyridinium tetrafluoroborate salts **9**-**11** was achieved in straightforward fashion upon treatment with $[Me_3O][BF_4]$. The longest-wavelength absorptions in the UV/visible spectra of **9**-**11** were all slightly red-shifted relative to their neutral counterparts (see ESI). The altered absorption was most pronounced in the 4- and 2-pyridyl TPVP salts **9** and **11**, which displayed longest-wavelength absorption at 363 nm and 369 nm, respectively. The effect of pyridine alkylation on the emission properties of **9**-**11**, however, was more significant. These compounds maintained fluorescence in the solid (aggregated) state as readily determined qualitatively by observing the emission of solid samples placed under a UV light. These materials also exhibited fluorescence emission in dilute solution, and the relative intensity of the fluorescence signal was virtually unaltered upon aggregation in each case. The emission spectra of **11** are representative (Fig. 4). This salt is readily dissolved in CH_2Cl_2 and the solution phase fluorescence spectrum revealed an emission signal at $\lambda_{max,em}$ = 456 nm. Incremental addition of hexane (a poor solvent for **11**) to the CH_2Cl_2 solution produced a series of emission spectra that were almost identical to the original.[27] The isomeric pyridinium salts **9** and **10** exhibited similar luminescent properties in CH_2Cl_2/hexane solution (see ESI). It seems that the AIE/AIEE effect has been switched off in tetraarylethylene derivatives **9**-**11** in favor of more or less constant fluorescence response irrespective of aggregation state. Thus, the neutral compounds **6**-**8** and their pyridinium derivatives **9**-**11** display two distinct fluorescent signatures.

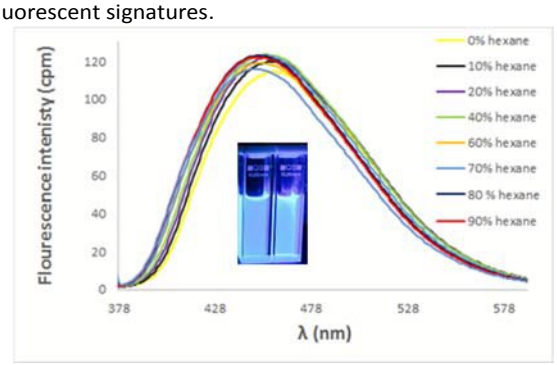

Fig. 4. Fluorescence spectra of **11** in CH_2Cl_2 and CH_2Cl_2/hexane mixtures ([**11**] = 10 μM, λ_{ex} = 369 nm). Inset: Picture taken under UV light of **11** in 100% CH_2Cl_2 (left) and 90:10 hexane:CH_2Cl_2 (right).

The dimethoxy analogue **14** was prepared to help demonstrate the versatility of double-Suzuki reactions for the preparation of functionalized tetraarylethylenes. Additionally, incorporation of two 4-methoxyphenyl groups into the TPVP framework provides a derivative electronically distinct from the parent TPVP **6**. Consistent with the greater conjugation in **14**, the longest-wavelength absorption in the UV/visible spectrum was slightly red-shifted by ~ 23 nm (λ_{max} = 328 nm, see ESI) compared to **6**. The AIE properties of **14** were also examined in acetonitrile/H_2O solution, and the associated spectra are illustrated in Fig. 5a. This material exhibited a fluorescence signal at $\lambda_{max,em}$ = 384 nm in pure CH_3CN. Incremental addition of H_2O initially produced an enhanced fluorescence emission at the same wavelength up to 60% H_2O. Further addition of H_2O, however, resulted first in slight bathochromic shift of the

emission wavelength, followed by diminished emission at 404 nm with concomitant increase in emission at significantly longer wavelength (490 nm). Such behavior in AIE-active systems may be attributed to subtle changes in the way that individual molecules are associated as a function of aggregation and solvent polarity.[11b,28] Red-shifted emission of **14** in solutions with high water content may reflect enhanced conjugation between the methoxyphenyl groups and the electron withdrawing pyridine ring. Additionally, longer wavelength emission upon increased aggregation may indicate charge transfer-type interactions between the electron-deficient pyridine ring and the electron-rich methoxyphenyl groups. Alkylation of the pyridine nitrogen gave the corresponding pyridinium salt (**15**). Not surprisingly, this salt exhibited a significant bathochromic shift in the absorption spectrum compared to the neutral precursor (λ_{max} = 441 nm). Pyridinium **15** also displayed observable fluorescence in dilute CH_2Cl_2 solution (Fig. 5b), as was the case with pyridinium TPVPs **9**-**11**. In contrast to **9**-**11**, however, incremental addition of hexane resulted in aggregation-caused quenching (ACQ) of this emission, in line with behavior observed for most organic fluorophores. We speculate that the combination of increased electron density in the methoxyphenyl groups with the known ability of N-alkylpyridinium salts to quench fluorescence of aromatic hydrocarbons may be responsible for this effect.[29]

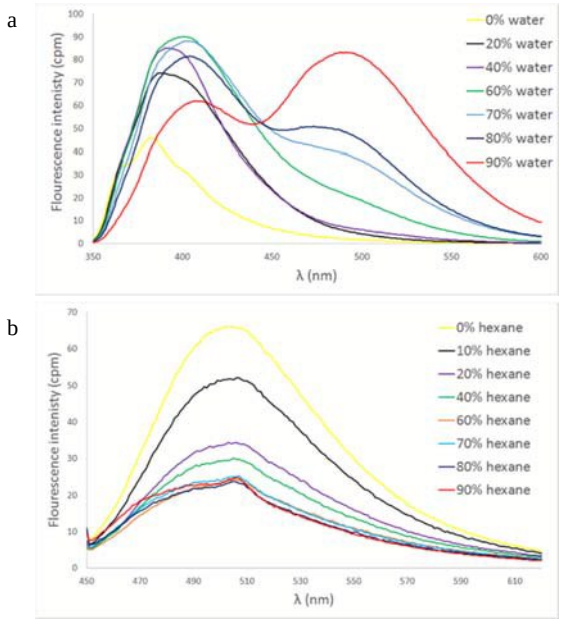

Fig. 5. (a) AIE effect revealed in fluorescence spectra of **14** in CH_3CN/H_2O mixtures ([**14**] = 10 μM, λ_{ex} = 328 nm). (b) ACQ effect shown in fluorescence spectra of **15** in CH_2Cl_2/hexane mixtures ([**15**] = 10 μM, λ_{ex} = 442 nm).

A switch to ACQ behavior was also observed in the fluorescence spectra of bis(pyridinium) salts **20**-**21**. While the neutral DPDPyE precursors **18** and **19** both displayed the expected AIE luminescence, conversion to the corresponding dications afforded salts that displayed fluorescence in dilute solution that became quenched upon aggregation. The fluorescence spectra of **19** and **21** shown in Fig. 6 provide representative illustrations of these phenomena.[30] The neutral DPDPyE **19** exhibits an AIE effect in CH_3CN/H_2O (Fig. 6a), while the initial fluorescence of the corresponding bis(pyridinium) salt **21** in CH_2Cl_2 is nearly completely quenched upon aggregation in 90% hexane. We ascribe the fluorescence quenching observed in **21** to the presence of two electron deficient N-methylpyridinium groups within the TAE framework, since incorporation of a single N-methylpyridinium group, as in **9**-**11**, fails to quench the inherent fluorescence. Similar spectra were observed in the 4-pyridyl isomers **18** and **20** (ESI).

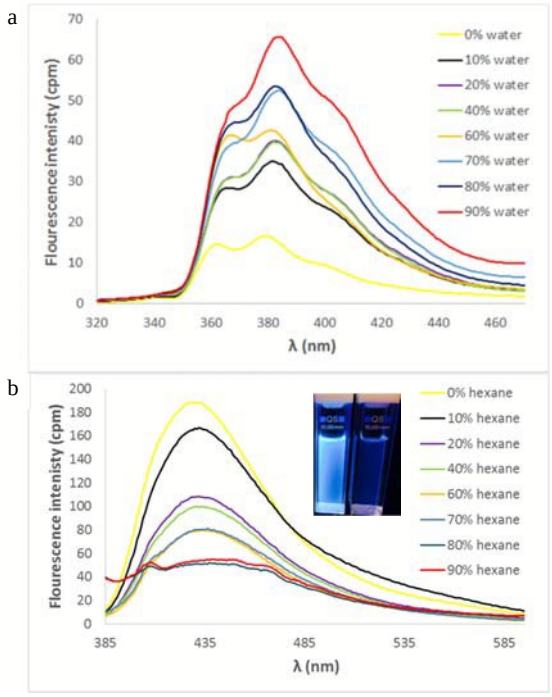

Fig. 6. (a) AIE effect in fluorescence spectra of DPDPyE **19** in CH_3CN/H_2O mixtures ([**19**] = 10 μM, λ_{ex} = 305 nm). (b) ACQ effect in fluorescence spectra of DPDPyE pyridnium salt **21** in CH_2Cl_2/hexane mixtures ([**21**] = 10 μM, λ_{ex} = 363 nm). Inset: Picture taken under UV light of **21** in 100% CH_2Cl_2 (left) and **21** in 90:10 hexane:CH_2Cl_2 (right).

A final class of TPVP derivative prepared and characterized as part of this study is shown in Scheme 4 and features two TPVP scaffolds linked through a common alkyl chain. Construction of **24** and **25** was easily achieved through prolonged heating of **6** and either 1,3-dichloropropane or 1,10-dibromodecane (2:1 molar ratio **6**:dihaloalkane) in CH_3CN. Potassium iodide was added to increase the reactivity of the haloalkane. The bis(TPVP) derivatives were ultimately isolated by column chromatography as iodide salts in good yield. The UV spectra of **24** and **25** both exhibited red-shifted longest wavelength absorptions relative to the TPVP precursor **6**, with **24** exhibiting a more pronounced shift (λ_{abs} = 390 nm) than **25** (λ_{abs} = 369 nm). The emission spectra in CH_2Cl_2 of both **24** and **25** revealed a fluorescence signal at similar λ_{max} (~459 nm) that was completely quenched upon addition of hexane, most likely due to the presence of iodide counterions.[31] Indeed, conversion of these linked TPVPs to the corresponding PF_6 salts **26** and **27** produced a fluorescence response in CH_2Cl_2/hexane that varied according to length of alkyl spacer. As shown in Fig. 7, addition

of hexane to a CH_2Cl_2 solution of **26** (three-carbon linker) elicited a diminution of fluorescence intensity (accompanied by a slight blue shift), similar to the behaviour of DPDPyE salts. In contrast, the fluorescence spectra of **27** (ten-carbon linker) in CH_2Cl_2 did not dramatically change upon addition of hexane, similar to the behaviour of N-methylpyridinium TPVP salt **9** (ESI).

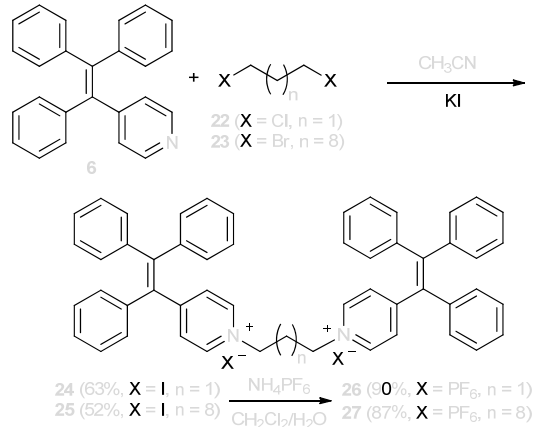

Scheme 4. Synthesis of alkyl-linked TPVP salts.

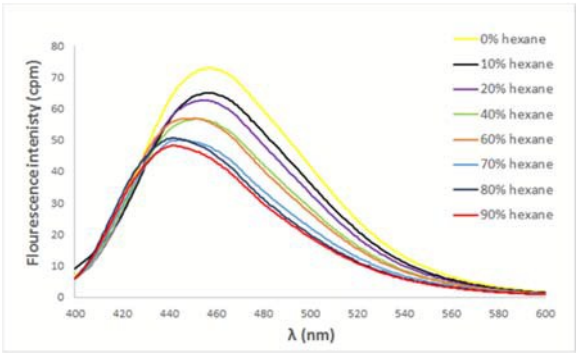

Fig. 7. Fluorescence spectra of **26** in CH_2Cl_2/hexane mixtures ([**26**] = 10 μM, λ_{ex} = 390 nm).

Conclusions

We have developed effective synthetic routes to novel tetraarylethylenes in which one or two of the core aryl rings have been replaced with heterocyclic (pyridine) groups. The tactics used to prepare these pyridine-containing TAEs also should be broadly applicable to the synthesis of other heterocyclic tetraarylethylenes incorporating alternative heteroarenes. The TPVP and DPDPyE derivatives **6**-**8**, **14**, and **18**-**19** function as AIE-luminogens, in keeping with their similarity to the prototypical AIE active compound tetraphenylethylene. Conversion of these materials to N-methyl pyridinium salts, however, results in divergent fluorescent properties. Specifically, mono-pyridinium salts **9**-**11** exhibit observable luminescence in both dilute solution and upon aggregation, while mono-pyridinium **15** and bis(pyridinium) salts **20**-**21** experience aggregation-caused quenching. Likewise, linking two TPVP frameworks with a short alkyl spacer also produces a fluorescent pyridinium salt that exhibits diminished emission upon aggregation. The ACQ effect in bis(TPVP) salts, however, is attenuated upon increasing the length of the alkyl spacer. The departure of these pyridinium-TAE salts from the typical AIE activity associated with closely related compounds indicates that additional factors other than restriction of intramolecular bond rotations influence the luminescence of these compounds. Nonetheless, the diverse fluorescence signatures observed in these pyridine/pyridinium-TAEs offer opportunities for developing new sensors and imaging agents based on turn-on or turn-off luminescence response. Currently, we are developing applications of (heteroaryl)arylethylenes along these lines while also examining the synthesis of additional heterocyclic analogues of TPE.

Experimental

General

All commercially available starting materials, reagents, and solvents were used as supplied, unless otherwise stated. Reactions were performed under inert atmosphere using solvents that were dried and purified by passage through activated alumina or activated molecular sieves. Reported yields are isolated yields. Purification of all final products was accomplished by silica gel flash column chromatography. Chloroform:methanol or hexane:ethyl acetate were used as elution solvents. Proton (^{1}H) and carbon (^{13}C) NMR were collected on Bruker NMR spectrometers at 300 MHz or 400 MHz for ^{1}H and 100 MHz or 75 MHz for ^{13}C. Chemical shifts (δ) are reported in parts-per million (ppm) relative to tetramethylsilane or residual undeuterated solvent. Melting points were recorded using a capillary melting point apparatus and are uncorrected. High resolution mass spectra were obtained in positive ion mode using electron spray ionization (ESI) on a double-focusing magnetic sector mass spectrometer. UV-Visible spectra were obtained using quartz cuvettes on a Varian Cary 100-Scan dual-beam spectrophotometer. Each measurement was done in duplicate and compared to solvent blank. Blank samples were prepared using HPLC grade acetonitrile or methylene chloride. Fluorescence spectra were obtained in air at room temperature using a Horiba Jobin Yvon Fluoromax-4 spectrofluorimeter using 3 mL quartz cuvettes. Samples were prepared using HPLC grade solvents. X-Ray diffraction data were collected on a Nonius Kappa CCD diffractometer equipped with Mo Kα radiation with λ = 0.71073 Å. Structures were solved by direct methods and data was refined by full-matrix least-squares refinement on F^2 against all reflections.

Synthetic Procedures

4-(1,2,2-Triphenylvinyl)pyridine (6)

A solution of benzhydryl(trimethyl)silane (2.88 g, 12.0 mmol, prepared according to the reported procedure.[22]) in 30 mL THF was cooled to 0 °C and n-BuLi (2.5 M solution in hexane, 4.0 mL, 10 mmol) was added via syringe. The resulting dark red solution was stirred at 0 °C for 2 h. 4-Benzoylpyridine (1.65 g, 9.00 mmol)

in 20 mL THF was added slowly to the reaction mixture. The reaction was then allowed to warm to room temperature and maintained overnight. The reaction was quenched with methanol and the solvent was evaporated to furnish an oily residue. The crude product was purified by flash column chromatography using ethyl acetate/hexane as eluent to yield TPVP **6** (1.92 g, 64%) as an off-white solid. M.p. 199-201 °C. ^{1}H NMR (300 MHz, $CDCl_3$) δ 6.91-7.15 (m, 17H), 8.34 (d, 2H, *J* = 5.9 Hz). ^{13}C NMR (100 MHz, $CDCl_3$) δ 127.1, 128.0, 128.1, 128.3, 128.8, 129.0, 129.1, 131.1, 132.2, 132.3, 139.3, 143.4, 143.7, 143.9, 144.7, 150.4, 152.8. HRMS (ESI): calcd for $C_{25}H_{20}N$ $[M+H]^+$, 334.1596; found, 334.1599.

3-(1,2,2-Triphenylvinyl)pyridine (7)

Using the procedure given above on 1.65 g (9.00 mmol) of 3-benzoylpyridine, TPVP **7** (1.77 g, 59%) was obtained initially as a reddish solid that was de-colorized by treatment with activated charcoal to afford a white solid. M.p. 156-159 °C. ^{1}H NMR (300 MHz, $CDCl_3$) δ 7.09-7.41 (m, 17H), 8.31 (s, 1H), 8.37(d, 1H, *J* = 5.1 Hz). ^{13}C NMR (75 MHz, $CDCl_3$) δ 125.3, 129.4, 129.5, 129.6, 130.4, 130.6, 130.7, 131.1, 133.8, 133.9, 134.0, 139.9, 140.9, 145.4, 145.5, 145.6, 145.7, 149.9, 154.6. HRMS (ESI): calcd for $C_{25}H_{20}N$ $[M+H]^+$, 334.1596; found, 334.1590.

2-(1,2,2-Triphenylvinyl)pyridine (8)

Using the procedure given above on 1.65 g (9.00 mmol) of 2-benzoylpyridine, TPVP **8** (2.01 g, 67%) was obtained as a white solid. M.p. 178-181 °C. ^{1}H NMR (300 MHz, DMSO-*d*6) δ 6.96-7.22 (m, 16H), 7.53-7.61 (m, 2H), 8.45 (d, 1H, *J* = 5.4 Hz). ^{13}C NMR (75 MHz, $CDCl_3$) δ 123.9, 129.1, 129.3, 129.4, 129.5, 130.3, 130.4, 130.6, 130.9, 133.7, 133.9, 138.1, 143.3, 144.8, 145.6, 145.8, 145.9, 152.1, 164.8. HRMS (ESI): calcd for $C_{25}H_{20}N$ $[M+H]^+$, 334.1596; found, 334.1598.

1-Methyl-4-(1,2,2-triphenylvinyl)pyridinium tetrafluoroborate (9)

Trimethyloxonium tetrafluoroborate (73 mg, 0.5 mmol) was added to a solution of **6** (100 mg, 0.3 mmol) in 25 mL of CH_2Cl_2 at 0 °C. The reaction was then allowed to warm to room temperature and monitored by TLC until disappearance of starting material was complete. The solvent was evaporated under reduced pressure and the residue was purified by flash column chromatography using methanol as eluent to give 96.5 mg (74%) of **9** as a yellow solid. M.p. 133-134 °C. ^{1}H NMR (300 MHz, $CDCl_3$) δ 4.28 (s, 3H), 7.02-7.41 (m, 17H), 8.37 (d, 2H, *J* = 6.2 Hz). ^{13}C NMR (100 MHz, $CDCl_3$) δ 48.9, 129.0, 129.2, 129.4, 129.9, 130.1, 130.2, 130.7, 132.1, 132.4, 132.5, 136.3, 141.5, 141.8, 142.4, 144.9, 151.4, 162.3. HRMS (ESI): calcd for $C_{26}H_{22}N$ $[M]^+$, 348.1752; found, 348.1766.

1-Methyl-3-(1,2,2-triphenylvinyl)pyridinium tetrafluoroborate (10)

Using the procedure given for the preparation of **9**, **7** (100 mg, 0.3 mmol) was converted to **10** (54.8 mg, 42%). M.p. > 200 °C. ^{1}H NMR (300 MHz, acetone-d_6) δ 3.87 (s, 3H), 7.31-7.68 (m, 15H), 8.29 (t, 1H), 8.61 (d, 1H, *J* = 6.9 Hz), 8.87 (s, 1H), 9.03 (d, 1H, *J* = 6.0 Hz). ^{13}C NMR (100 MHz, acetone-d_6) δ 48.8, 128.1, 128.6, 128.7, 128.9, 129.5, 129.6, 131.7, 132.2, 132.3, 134.9, 135.4, 140.4, 142.1, 142.5, 143.0, 144.2, 145.0, 147.8, 150.0. HRMS (ESI): calcd for $C_{26}H_{22}N$ $[M]^+$, 348.1752; found, 348.1758.

1-Methyl-2-(1,2,2-triphenylvinyl)pyridinium tetrafluoroborate (11)

Using the procedure given for the preparation of **9**, **8** (100 mg, 0.3 mmol) was converted to **11** (79.6 mg, 61%). M.p. 150-153 °C. ^{1}H NMR (300 MHz, acetone-d_6) δ 4.36 (s, 3H), 7.19-7.34 (m, 16H), 7.97-8.15 (m, 2H) 8.78 (d, 1H, *J* = 5.1 Hz). ^{13}C NMR (75 MHz, acetone-d_6) δ 49.8, 130.7, 130.8, 131.1, 131.3, 131.4, 132.4, 133.2, 133.4, 133.5, 133.6, 133.9, 141.5, 143.4, 143.7, 144.4, 147.8, 149.4, 153.8, 158.1. HRMS (ESI): calcd for $C_{26}H_{22}N$ $[M]^+$, 348.1752; found, 348.1755.

4-(2,2-Dibromo-1-phenylvinyl)pyridine (13)

4-Benzoylpyridine (182 mg, 1.00 mmol) was dissolved in chlorobenzene (50 mL). Carbon tetrabromide (662 mg, 2.00 mmol) and PPh_3 (1.05 g, 4.00 mmol) were added and the reaction mixture was heated to reflux and maintained for 3 d. After this time the reaction mixture was allowed to cool to rt and insoluble material was removed by filtration. The filtrate was treated with 50 mL of 1 M aq. HCl. The aqueous layer was separated and basified with 1 M aq. NaOH until pH 12. The aqueous phase was extracted with CH_2Cl_2 (2 × 50 mL), and the combined organic fractions were dried over anhydrous Na_2SO_4, filtered, and concentrated under reduced pressure. The crude product was purified by flash column chromatography using ethyl acetate/hexane as eluent to yield **13** (162 mg, 48%) as a buff solid. M.p. 109-112 °C. ^{1}H NMR (300 MHz, $CDCl_3$) δ 7.26-7.43 (m, 7H), 8.65 (d, 2H, *J* = 5.2 Hz). ^{13}C NMR (100 MHz, $CDCl_3$) δ 93.4, 124.5, 129.6, 129.7, 129.8, 141.1, 146.4, 149.9, 151.1. HRMS (ESI): calcd for $C_{13}H_{10}Br_2N$ $[M+H]^+$, 337.9180; found, 337.9182.

4-(2,2-Bis(4-methoxyphenyl)-1-phenylvinyl)pyridine (14)

Compound **13** (338 mg, 1.00 mmol) was dissolved in 50 mL of dioxane:water (4:1). The flask was charged with Na_2CO_3 (690 mg, 5.00 mmol), $Pd(OAc)_2$ (28 mg, 0.12 mmol), PPh_3 (130 mg, 0.50 mmol), and 4-methoxyphenylboronic acid (760 mg, 5.00 mmol). The reaction mixture was heated to reflux overnight. After cooling to rt, the reaction mixture was extracted with ethyl acetate (3 × 50 mL) and the combined organic fractions were dried over anhydrous Na_2SO_4, filtered, and concentrated under reduced pressure. The crude product was purified by flash column chromatography using ethyl acetate/hexane as eluent to yield 271 mg (69%) of **14** as a creamy white solid. M.p. 174-176 °C. ^{1}H NMR (400 MHz, $CDCl_3$) δ 3.74 (s, 3H), 3.78 (s, 3H), 6.63-6.68 (m, 4H), 6.91-7.15 (m, 11H), 8.33 (d, 2H, *J* = 6.1 Hz). ^{13}C NMR (100 MHz, $CDCl_3$) δ 56.1, 56.2, 114.1, 114.4, 115.8, 117.2, 127.1, 127.7, 129.1, 132.3, 133.6, 136.2, 136.4, 137.4, 143.9, 150.3, 153.4, 159.6, 159.9. HRMS (ESI): calcd for $C_{27}H_{24}NO_2$ $[M+H]^+$, 394.1807; found, 394.1810. X-Ray quality crystals of **14** were grown by slow evaporation of EtOAC/MeOH solution at rt.

1-Methyl-4-(2,2-bis(4-methoxyphenyl)-1-phenylvinyl)pyridinium tetrafluoroborate (15)

Using the procedure for the preparation of **9** given above, 118 mg (0.30 mmol) **14** was converted to **15** (90.7 mg, 63%). M.p. 169-171 °C. ^{1}H NMR (400 MHz, acetone-d_6) δ 3.72 (s, 3H), 3.78 (s, 3H), 4.43 (s, 3H), 6.70-7.23 (m, 13H), 7.52 (d, 2H, *J* = 7.0 Hz), 8.84 (d, 2H, *J* = 6.9 Hz). ^{13}C NMR (100 MHz, acetone-d_6) δ 48.6, 55.9, 56.1, 114.3, 115.2, 128.6, 129.6, 130.3, 132.6, 133.7, 134.2, 134.6, 135.1, 135.3, 142.9, 145.6, 149.8, 160.6, 161.1, 162.5. HRMS (ESI): calcd for $C_{28}H_{26}NO_2$ $[M]^+$, 408.1964; found, 408.1952.

4,4'-(2,2-diphenylethene-1,1-diyl)dipyridine (18)

Dibromoethene **16**[25] (338 mg, 1.00 mmol) was dissolved in 50 mL of dioxane:water (4:1). The flask was charged with Na_2CO_3 (690 mg, 5.00 mmol), $Pd(OAc)_2$ (28 mg, 0.12 mmol), PPh_3 (130 mg, 0.50 mmol) and 4-pyridine boronic acid **17a** (615 mg, 5.00 mmol). The reaction was heated to reflux under argon overnight. After colling, the reaction mixture was extracted with ethyl acetate (3 × 50 mL) and the combined organic fractions were dried over anhydrous Na_2SO_4, filtered, and concentrated under reduced pressure. The crude product was purified by flash column chromatography using ethyl acetate/hexane as eluent to yield **18** (183 mg, 55%) as a creamy white solid. M.p. 162-165 °C. ^{1}H NMR (300 MHz, $CDCl_3$) δ 6.95 (d, 4H, *J* = 6.0 Hz), 7.06-7.09 (m, 4H), 7.19-7.26 (m, 6H), 8.43 (d, 4H, *J* = 6.0 Hz). ^{13}C NMR (75 MHz, $CDCl_3$) δ 124.1, 128.4, 130.5, 130.8, 133.5, 144.4, 148.4, 152.3, 152.8. HRMS (ESI): calcd for $C_{24}H_{19}N_2$ $[M+H]^+$, 335.1548; found, 335.1555. X-Ray quality crystals of **18** were grown by slow evaporation of EtOAc/MeOH solution at rt.

3,3'-(2,2-diphenylethene-1,1-diyl)dipyridine (19)

Using the procedure for the preparation of **18** given above and substitution of 3-pyridine boronic acid (**17b**) in place of **17a**, DPDPyE **19** (207 mg, 62%) was obtained as a white solid. M.p. 159-161 °C. ^{1}H NMR (300 MHz, $CDCl_3$) δ 7.06-7.20 (m, 5H), 7.47-7.75 (m, 9H), 8.31 (s, 2H), 8.39 (d, 2H, *J* = 4.9 Hz). ^{13}C NMR (75 MHz, $CDCl_3$) δ 125.5, 130.8, 131.1, 131.2, 133.8, 134.7, 134.8, 140.8, 144.8, 150.4, 154.5. HRMS (ESI): calcd for $C_{24}H_{19}N_2$ $[M+H]^+$, 335.1548; found, 335.1553.

4,4'-(2,2-diphenylethene-1,1-diyl)bis(1-methylpyridinium) bis(tetrafluoroborate) (20)

A mixture of trimethyloxonium tetrafluoroborate (219 mg, 1.50 mmol) and **18** (100 mg, 0.30 mmol) in 25 mL MeOH was heated to reflux for 5 d. The crude product was purified by flash column chromatography using methanol as eluent to yield **20** (109 mg, 72%) as an orange solid. M.p. 139-141 °C. ^{1}H NMR (400 MHz, DMSO-d_6) δ 4.24 (s, 6H), 7.12-7.34 (m, 10H), 7.72 (d, 4H, *J* = 6.8 Hz), 8.82 (d, 4H, *J* = 6.5 Hz). ^{13}C NMR (75 MHz, DMSO-d_6) δ 50.7, 129.2, 131.8, 132.7, 134.1, 136.3, 142.8, 148.2, 156.1, 159.6. HRMS (ESI): calcd for $C_{13}H_{12}N$ $[M]^{2+}/2$, 182.0969; found, 182.0973.

3,3'-(2,2-diphenylethene-1,1-diyl)bis(1-methylpyridinium) bis(tetrafluoroborate) (21)

Using the procedure given for the preparation of **20**, 100 mg **19** was converted to bis(pyridinium) salt **21** (88.3 mg, 58%). M.p. 164-167 °C. ^{1}H NMR spectrum: (300 MHz, acetone-d_6) δ 4.38 (s, 6H), 7.27-7.39 (m, 10H), 8.07-8.19 (m, 2H), 8.68 (d, 2H, *J* = 6.9 Hz), 8.89 (s, 2H), 8.93 (d, 2H, *J* = 5.6 Hz). ^{13}C NMR (100 MHz, acetone-d_6) δ 49.2, 128.5, 129.7, 129.8, 132.1, 133.0, 133.1, 133.8, 141.2, 142.0, 144.9, 150.6. HRMS (ESI): calcd for $C_{13}H_{12}N$ $[M]^{2+}/2$, 182.0969; found, 182.0971.

1,1'-(Propane-1,3-diyl)bis(4-(1,2,2-triphenylvinyl)pyridinium) diiodide (24)

Compound **6** (134 mg, 0.40 mmol), KI (66.4 mg, 0.40 mmol), and 1,3-dichloropropane (22.4 mg, 0.20 mmol) were combined in 50 mL CH_3CN and heated to reflux for 6-7 d. After this time the solvent was evaporated and the residue purified by flash column chromatography using methanol as the eluent to afford **24** (121 mg, 63%) as a yellow-orange solid. M.p. 135-138 °C. ^{1}H NMR (300 MHz, methanol-d_4) δ 2.07-2.13 (m, 2H), 4.73 (t, 4H, *J* = 7.2 Hz), 7.08-7.36 (m, 30H), 7.62 (d, 4H, *J* = 6.8 Hz), 8.81 (d, 4H, *J* = 6.9 Hz). ^{13}C NMR (100 MHz, $CDCl_3$) δ 30.7, 56.2, 129.1, 129.4, 129.6, 130.1, 130.2, 130.7, 130.8, 130.9, 132.1, 132.3, 132.5, 141.4, 141.6, 142.1, 144.4, 152.4, 163.3. HRMS (ESI): calcd for $C_{53}H_{44}N_2I$ $[M]^+$, 835.2549; found, 835.2559.

1,1'-(Decane-1,10-diyl)bis(4-(1,2,2-triphenylvinyl)pyridinium) diiodide (25)

Using the procedure given above and 1,10-dibromodecane (60 mg, 0.20 mmol) in place of dichloropropane, **25** (110 mg, 52%) was obtained as a yellow solid. M.p. 186-189 °C. ^{1}H NMR (300 MHz, acetone-d_6) δ 1.22-1.41 (m, 16H), 4.86 (t, 4H, *J* = 7.3 Hz), 7.13-7.34 (m, 30H), 7.71 (d, 4H, *J* = 5.9 Hz), 9.27 (d, 4H, *J* = 6.6 Hz). ^{13}C NMR (100 MHz, acetone-d_6) δ 26.3, 29.4, 30.3, 32.1, 61.2, 128.8, 128.9, 129.4, 129.5, 129.6, 129.7, 130.5, 131.9, 132.3, 132.4, 137.3, 141.9, 142.4, 142.9, 145.5, 149.3, 161.8. HRMS (ESI): calcd for $C_{30}H_{29}N$ $[M]^{2+}/2$, 403.2300; found, 403.2297.

Hexafluorophosphate salts 26 and 27

The preparation of **26** is representative. Diiodide salt **24** (51 mg, 0.052 mmol) was dissolved in 5 mL CH_2Cl_2. A solution of saturated aq. NH_4PF_6 (25 mL) was added and the biphasic mixture was vigorously stirred at rt overnight. The layers were separated and the organic phase was dried over anhydrous Na_2SO_4, filtered, and concentrated to afford **26** (47 mg, 90%) as a yellow-orange solid. M.p. 204-207 °C. Negative ion LRMS (ESI) confirmed the presence of PF_6 (*m/z* = 145) and the absence of iodide. In similar fashion, **25** (62 mg, 0.058 mmol) was converted to **27** (55 mg, 87%). M.p. 165-168 °C.

Acknowledgments

We thank the Department of Chemistry, University of Iowa and the UI Graduate College for a Radiochemistry Summer Fellowship (M.G.). We also thank Dale C. Swenson and Christopher J. Kassl for assistance with X-ray crystallography.

Notes and references

1 (a) S. W. Yun, N. Y. Kang, S. J. Park, H. H. Ha, Y. K. Kim, J. S. Lee and Y. T. Chang, *Acc. Chem. Res.*, 2014, **47**, 1277-1286. (b) J. Chan, S. C. Dodani and C. J. Chang, *Nat. Chem.*, 2012, **4**, 973-984. (c) H. Kobayashi, M. Ogawa, R. Alford, P. L. Choyke and Y. Urano, *Chem. Rev.*, 2010, **110**, 2620-2640. (d) L. D. Lavis and R. T. Raines, *ACS Chem. Biol.*, 2008, **3**, 142-155.

2 (a) B. Rout, L. Motiei and D. Margulies, *Synlett*, 2014, 1050-1054. (b) K. P. Carter, A. M. Young and A. E. Palmer, *Chem. Rev.*, 2014, **114**, 4564-4601. (c) M. Zhu and C. Yang, *Chem. Soc. Rev.*, 2013, **42**, 4963-4976.

3 (a) Y. Hong, J. W. Y. Lam and B. Z. Tang, *Chem. Commun.*, 2009, 4332-4353. (b) J. Mei, Y. Hong, J. W. Y. Lam, A. Qin, Y. Tang and B. Z. Tang, *Adv. Mater.*, 2014, **26**, 5429-5479.

4 (a) J. Liang, B. Z. Tang and B. Liu, *Chem. Soc. Rev.*, 2015, **44**, 2798-2811. (b) D. Ding, K. Li, B. Liu and B. Z. Tang, *Acc. Chem. Res.*, 2013, **46**, 2441-2453. (c) Y. Hong, J. W. Y. Lam and B. Z. Tang, *Chem. Soc. Rev.*, 2011, **40**, 5361-5388. (d) M. Wang, G. Zhang, D. Zhang, D. Zhu and B. Z. Tang, *J. Mater. Chem.*, 2010, **20**, 1858-1867.

5 N. L. C. Leung, N. Xie, W. Yuan, Y. Liu, Q. Wu, Q. Peng, Q. Miao, J. W. Y. Lam and B. Z. Tang, *Chem. – Eur. J.*, 2014, **20**, 15349-15353.

6 F. Hu, Y. Huang, G. Zhang, R. Zhao and D. Zhang, *Tetrahedron Lett.*, 2014, **55**, 1471-1474.

7 F. Hu, G. Zhang, C. Zhan, W. Zhang, Y. Yan, Y. Zhao, H. Fu and D. Zhang, *Small*, 2015, **11**, 1335-1344.

8 X. Chen, X. Y. Shen, E. Guan, Y. Liu, A. Qin, J. Z. Sun and B. Z. Tang, *Chem. Commun.*, 2013, **49**, 1503-1505.

9 H. R. Xu, K. Li, S. Y. Jiao, S. L. Pan, J. R. Zeng and X. Q. Yu, *Analyst*, 2015, **140**, 4182-4188.

10 (a) Y. Yuan, Y. Chen, B. Z. Tang and B. Liu, *Chem. Commun.*, 2014, **50**, 3868-3870. (b) H. Shi, N. Zhao, D. Ding, J. Liang, B. Z. Tang and B. Liu, *Org. Biomol. Chem.*, 2013, **11**, 7289-7296.

11 (a) W. Zhang, R. T. K. Kwok, Y. Chen, S. Chen, E. Zhao, C. Y. Y. Yu, J. W. Y. Lam, Q. Zheng and B. Z. Tang, *Chem. Commun.*, 2015, **51**, 9022-9025. (b) N. Zhao, M. Li, Y. Yan, J. W. Y. Lam, Y. L. Zhang, Y. S. Zhao, K. S. Wong and B. Z. Tang, *J. Mater. Chem. C*, 2013, **1**, 4640-4646.

12 D. Y. Chen, J. B. Shi, Y. M. Yu, B. Tong, J. G. Zhi and Y. P. Dong, *Sci. China Chem.*, 2013, **56**, 1239-1246.

13 T. Hu, B. Yao, X. Chen, W. Li, Z. Song, A. Qin, J. Z. Sun and B. Z. Tang, *Chem. Commun.*, 2015, **51**, 8849-8852.

14 (a) X. Yao, X. Ma and H. Tian, *J. Mater. Chem. C*, 2014, **2**, 5155-5160. (b) P. P. Kapadia, J. C. Widen, M. A. Magnus, D. C. Swenson, and F. C. Pigge, *Tetrahedron Lett.*, 2011, **52**, 2519-2522. (c) P. P. Kapadia, M. A. Magnus, D. C. Swenson and F. C. Pigge, *J. Mol. Struct.*, 2011, **1003**, 82-86.

15 F. C. Pigge, *J. Mol. Eng. Mater.*, 2013, **1**, 1340009 (14 pages).

16 G. Huang, G. Zhang and D. Zhang, *Chem. Commun.*, 2012, **48**, 7504-7506.

17 F. C. Pigge, P. P. Kapadia and D. C. Swenson, *CrystEngComm*, 2013, **15**, 4386-4391.

18 (a) X. Yan, T. R. Cook, P. Wang, F. Huang and P. J. Stang, *Nat. Chem.*, 2015, **7**, 342-348. (b) Q. Gong, Z. Hu, B. J. Deibert, T. J. Emge, S. J. Teat, D. Banerjee, B. Mussman, N. D. Rudd and J. Li, *J. Am. Chem. Soc.*, 2014, **136**, 16724-16727. (c) B. Icli, E. Solari, B. Kilbas, R. Scopelliti and K. Severin, *Chem. – Eur. J.*, 2012, **18**, 14867-14874.

19 B. Kilbas, S. Mirtschin, R. Scopelliti and K. Severin, *Chem. Sci.*, 2012, **3**, 701-704.

20 A. Richardson, Jr., J. B. Choudary and D. E. Holtkamp, *J. Med. Chem.*, 1975, **18**, 689-691.

21 (a) K. Garg, E. Ganapathi, P. Rajakannu and M. Ravikanth, *Phys. Chem. Chem. Phys.*, 2015, **17**, 19465-19473. (b) E. Zhao, H. Deng, S. Chen, Y. Hong, C. W. T. Leung, J. W. Y. Lam and B. Z. Tang, *Chem. Commun.*, 2014, **50**, 14451-14454. (c) A. Bolzoni, L. Viglianti, A. Bossi, P. R. Mussini, S. Cauteruccio, C. Baldoli and E. Licandro, *Eur. J. Org. Chem.*, 2013, 7489-7499. (d) D. Jana and B. K. Ghorai, *Tetrahedron*, 2012, **68**, 7309-7316. (e) X. F. Duan, J. Zeng, J. W. Lü and Z. B. Zhang, *Synthesis*, 2007, 713-718.

22 N. S. Mills, C. Tirla, M. A. Benish, A. J. Rakowitz, L. M. Bebell, C. M. M. Hurd and A. L. M. Bria, *J. Org. Chem.*, 2005, **70**, 10709-10716.

23 M. Banerjee, S. J. Emond, S. V. Lindeman and R. Rathore, *J. Org. Chem.*, 2007, **72**, 8054-8061.

24 (a) G. F. Zhang, Z. Q. Chen, M. P. Aldred, Z. Hu, T. Chen, Z. Huang, X. Meng and M. Q. Zhu, *Chem. Commun.*, 2014, **50**, 12058-12060. (b) G. F. Zhang, H. Wang, M. P. Aldred, T. Chen, Z. Q. Chen, X. Meng and M. Q. Zhu, *Chem. Mater.*, 2014, **26**, 4433-4446.

25 J. C. Barnes, M. Juríček, N. L. Strutt, M. Frasconi, S. Sampath, M. A. Giesener, P. L. McGrier, C. J. Bruns, C. L. Stern, A. A. Sarjeant and J. F. Stoddart, *J. Am. Chem. Soc.*, 2013, **135**, 183-192.

26 These structures have been deposited with the Cambridge Crystallographic Database, **14**: CCDC# 1421838; **18**: CCDC# 1421839. See ESI for crystallographic data.

27 This solvent combination has been used to probe for AIE activity in other N-methylpyridinium TPE derivatives, see reference 7.

28 Z. Wang, J. H. Ye, J. Li, Y. Bai, W. Zhang and W. He, *RSC Adv.*, 2015, **5**, 8912-8917.

29 G. A. Davis, *J. Chem. Soc., Chem. Commun.*, 1973, 728-729.

30 The effect of f_{hexane} > 90% on the fluorescence of **20** and **21** was qualitatively examined, however no enhanced emission was observed at higher hexane content.

31 The fluorescence quenching effect of iodide is well known and has been observed in other TPE derivatives, cf. references 7 and 9.